이학석사학위논문

Hydrogen Storage in Grahene Oxide Layers: First-Principles Study and Monte Carlo Simulations

산화그래핀층에서 수소저장: 제일원리계산과 몬테카를로 시뮬레이션

2015년 2월

서울대학교 대학원

물리천문학부

문 효 원

Hydrogen Storage in Grahene Oxide Layers: First-Principles Study and Monte Carlo Simulations

산화그래핀층에서 수소저장: 제일원리계산과 몬테카를로 시뮬레이션

지도교수 임 지 순

이 논문을 이학석사 학위논문으로 제출함

2015년 2월

서울대학교 대학원

물리천문학부

문 효 원

문효원의 이학석사 학위논문을 인준함

2014년 12월

위 원 장 최 무 영 (인)

부위원장 임 지 순 (인)

위 원 정 현 석 (인)

Hydrogen Storage in Grahene Oxide Layers: First-Principles Study and Monte Carlo Simulations

Hyo-Won Moon

supervised by

Professor Jisoon Ihm

A Dissertation
Submitted to the Faculty of
Seoul National University
in Partial Fulfillment of
the Requirements for the Degree of
Master of Philosophy

December 2014

Department of Physics and Astronomy
Graduate School
Seoul National University

Abstract

Concerning the depletion of fossil fuels and environmental pollutions by them, new energy sources have been vastly investigated. Among these new energy sources, hydrogen energy is one of the most promising because they can be easily obtained from water around us and they don't produce polluting materials. However, the biggest problem to use the hydrogen energy is safe and high-capacity storage of them.

Graphene as 2-dimensional material composed of carbon has distinct feature like high electric and heat conductivity, and high strength. So many people have researched it. In this study, I simulated how much hydrogen gas are stored in two systems that are graphene layers and graphene oxide layers where oxygens are attached as epoxy group, and then I investigated the oxygen effect.

I used two calculation tools. The first is ab-initio calculation, also known as first-principles study using density functional theory. The second is Monte Carlo simulation using metropolis algorithm. For ab-initio calculations, I used VASP(Vienna Abinitio Simulation Package) adopting PBE(Perdew, Burke and Ernzerhof) functional and for the Monte Carlo simulations, I made a program using Fortran 90.

Here is the calculation procedures. First, I got the H_2-H_2 interaction energy using VASP, changing their relative distance. As

H_2 is a diatomic molecule, there also is angle dependence of the energy. However, I ignored the angle dependence by calculating H_2-H_2 interaction for 4 most symmetric configurations and thermally averaging them in the reason that including the angle dependence increases calculation cost too much and it seems that including the angle dependence doesn't make a big difference.

Second, I got the potential energy field in graphene layers and graphene oxide layers from total energy differences between whether one H_2 molecule is in the systems or not. I also used VASP to get the potential energy fields. In these cases, I also ignore the angle dependence of H_2 like H_2-H_2 interaction case. In these cases, I arranged H_2 molecule in three axis directions of the systems.

Lastly, using the informations obtained above, I simulated Monte Carlo simulations. It show that the oxygen increases the potential energy in the vicinity of oxygen, but decreases the potential energy in the other region. Put together, I concluded the oxygen interrupts hydrogen storage in the system.

keywords : Hydrogen Storage, Graphene, Graphene Oxide, Monte Carlo Simulation, Density Functional Theory
Student Number : 2013-20366

Contents

Chapter 1
Introduction

With the increasing interest of hydrogen energy, many people try to substitute the fossil fuels to the hydrogen energy. Some company commercialized the hydrogen car that use hydrogen as fuel. However, they use high pressure tank for hydrogen storage and there are dangers of explosion. In this study, I examined the graphene layers and graphene oxide layers as hydrogen storage materials, and investigated the effect of oxygen.

In chapter 2, I'll overview the basic theory for the study, density functional theory and Monte Carlo simulation. To arrive the density functional theory, we need to adopt some approximations and restrict our system. Monte Carlo simulations for systems in thermal equilibrium, use metropolis algorithm. There are two ways for the Monte Carlo simulations; canonical ensemble and grand canonical ensemble. The former fixes the number of particle and the latter varies the number of particles. In this study, I made the program for the canonical ensemble.

In chapter 3, I will show my calculation results. There are two kind of DFT calculation. One is H_2-H_2 interaction energy calculation. The other is potential energy field calculation. As H_2 is a diatomic

molecule, hydrogen's angle dependence exists. However, including the angle dependence increases calculation cost too much and it seems that including the angle dependence doesn't make a critical difference. So I averaged out the angle dependence over some angles.

In chapter 4, I'll show the calculation details adopted in VASP; energy cutoff, k sampling method, the number of k-points, the functional used, smearing method and etc options. Also I'll will show the details used in Monte Carlo simulations.

Finally, in chapter 5 I'll summarize and conclude my study.

Chapter 2
Basic Theory

2.1 Many-Body Schrodinger's Equation

To describe a particle quantum mechanically, we need to solve the Schrodinger's Equation

$$i\hbar\frac{\partial}{\partial t}\Psi(\vec{r},t)=\left[-\frac{\hbar^2}{2m}\nabla^2+V(\vec{r})\right]\Psi(\vec{r},t) \tag{2.1}$$

we can exactly solve the equation at least numerically. But as the particle's number increases, the equation becomes very complicate.

$$i\hbar\frac{\partial}{\partial t}\Psi(\vec{r_1},...,\vec{r_N},t)=\left[-\sum_{i=1}^{N}\frac{\hbar^2}{2m_i}\nabla_i+V(\vec{r_1},...,\vec{r_N})\right]\Psi(\vec{r_1},...,\vec{r_N},t) \tag{2.2}$$

This is the many-body Schrodinger's equation of N particle. Where $\vec{\underline{r}}\equiv\{\vec{r_i}:\ i=1,...,N\}$ is the coordinate of particles, m_i is the mass of ith particle and $V(\vec{r_1},...,\vec{r_N})$ is the potential energy when the particles located at $\vec{r_1},...,\vec{r_N}$. As the number of mole-order particles are contained in macroscopic matter, solving the Schrodinger's equation for macroscopic matters requires the solution of differential equation with mole-order variables. Therefore, we can't solve the equation in general. We need to adopt some approximations and restrict our systems to solve the many-body Schrodinger's equation practically.

2.2 Born-Oppenheimer Approximation

For the system composed of electrons and nucleus, the hamiltonian becomes

$$\hat{H}=-\sum_{I=1}^{P}\frac{\hbar^2}{2M_I}\nabla_I^2-\sum_{i=1}^{N}\frac{\hbar^2}{2m}\nabla_i^2+\frac{e^2}{2}\sum_{I=1}^{P}\sum_{J\neq I}^{P}\frac{Z_I Z_J}{\left|\overrightarrow{R_I}-\overrightarrow{R_J}\right|}$$
$$+\frac{e^2}{2}\sum_{i=1}^{N}\sum_{j\neq i}^{N}\frac{1}{\left|\overrightarrow{r_i}-\overrightarrow{r_j}\right|}-e^2\sum_{I=1}^{P}\sum_{i=1}^{N}\frac{Z_I}{\left|\overrightarrow{R_I}-\overrightarrow{r_i}\right|} \tag{2.3}$$

where P is the number of nuclei, N is the number of electrons, M_I is the mass of Ith nucleus, m is the mass of electrons, $\underline{\overrightarrow{R}}\equiv\left\{\overrightarrow{R_I}:I=1,...,P\right\}$ is the coordinates of nuclei, $\underline{\overrightarrow{r}}\equiv\left\{\overrightarrow{r_i}:I=1,...,N\right\}$ is the coordinates of electrons and Z_I is the charge of Ith nucleus. The first and second terms mean nuclei's kinetic energy and electrons' kinetic energy, respectively. The third, fourth and fifth term mean nucleus-nucleus interaction energy, electron-electron interaction energy and electron-nucleus interaction energy, respectively. Thus the Schrodiger's equation becomes

$$i\hbar\frac{\partial}{\partial t}\Psi(\underline{\overrightarrow{R}},\underline{\overrightarrow{r}},t)=\hat{H}\Psi(\underline{\overrightarrow{R}},\underline{\overrightarrow{r}},t) \tag{2.4}$$

If we assume the adiabatic approximation, that is electrons follow nuclei instantaneously while keeping their eigenstates, we can construct the form of the solution

$$\Psi(\underline{\overrightarrow{R}},\underline{\overrightarrow{r}},t)=\sum_n\Theta_n(\underline{\overrightarrow{R}},t)\Phi_n(\underline{\overrightarrow{R}},\underline{\overrightarrow{r}}) \tag{2.5}$$

Now, we can decompose the Schrodinger's equation

$$\left[-\sum_{i=1}^{N}\frac{\hbar^2}{2m}\nabla_i^2+\frac{e^2}{2}\sum_{i=1}^{N}\sum_{j\neq i}^{N}\frac{1}{\left|\overrightarrow{r_i}-\overrightarrow{r_j}\right|}-e^2\sum_{I=1}^{P}\sum_{i=1}^{N}\frac{Z_I}{\left|\overrightarrow{R_I}-\overrightarrow{r_i}\right|}\right]\Phi_n(\underline{\overrightarrow{R}},\underline{\overrightarrow{r}})$$
$$=E_n(\underline{\overrightarrow{R}})\Phi_n(\underline{\overrightarrow{R}},\underline{\overrightarrow{r}}) \tag{2.6}$$

$$\left[i\hbar\frac{\partial}{\partial t}+\sum_{I=1}^{P}\frac{\hbar^2}{2M_I}\nabla_I^2-\frac{e^2}{2}\sum_{I=1,J\neq I}^{P}\sum^{P}\frac{Z_IZ_J}{\left|\overrightarrow{R_I}-\overrightarrow{R_J}\right|}-E_q(\vec{R})\right]\Theta_q(\vec{\underline{R}},t)=$$

$$-\sum_n\sum_{I=1}^{P}\frac{\hbar^2}{2M_I}\langle\Phi_q|\nabla_I^2|\Phi_n\rangle\Theta_n(\vec{\underline{R}},t)-2\sum_n\sum_{I=1}^{P}\frac{\hbar^2}{2M_I}\nabla_I\Theta_n(\vec{\underline{R}},t)\cdot\langle\Phi_q|\nabla_I|\Phi_n\rangle \tag{2.7}$$

From equation (2.7), we can see that to validate the approximation, the off-diagonal terms can be neglected. If we neglect them, the equation (2.7) becomes

$$i\hbar\frac{\partial}{\partial t}\Theta_q(\vec{\underline{R}},t)=$$

$$\left[-\sum_{I=1}^{P}\frac{\hbar^2}{2M_I}\nabla_I^2+E_q(\vec{\underline{R}})+\frac{e^2}{2}\sum_{I=1,J\neq I}^{P}\sum^{P}\frac{Z_IZ_J}{\left|\overrightarrow{R_I}-\overrightarrow{R_J}\right|}+\sum_{I=1}^{P}\frac{\hbar^2}{2M_I}\langle\Phi_q|\nabla_I^2|\Phi_q\rangle\right]\Theta_q(\vec{\underline{R}},t) \tag{2.8}$$

Frequently, the last term in right side is neglected because usually

$$\sum_{I=1}^{P}\frac{\hbar^2}{2M_I}\langle\Phi_q|\nabla_I^2|\Phi_q\rangle=\frac{m}{M_I}\sum_{I=1}^{P}\left(\frac{\hbar^2}{2m}\langle\Phi_q|\nabla_I^2|\Phi_q\rangle\right)\sim\frac{m}{M}E_q(\vec{\underline{R}}) \tag{2.9}$$

Where M is proton's mass. In that case, It is called Born-Oppenheimer approximation. Frequently, Born-Oppenheimer approximation is used to indicate the adiabatic approximation.

2.3 Electronic Structure

If we consider the equation (2.6), it's called electronic structure problem. Ab-initio calculation, also known as first-principles calculation is named for the calculation of the problem because the equation contains no empirical parameters. Therefore, without any experiment we can analyze some systems' properties. In the other word, the properties come from pure quantum mechanical theory. There are two representative method to solve the equation.

2.3.1 Hartree-Fock Method

This method assumes the form of the solution

$$\Phi_{HF}(\vec{x_1},...,\vec{x_N}) = \frac{1}{\sqrt{N!}} \begin{vmatrix} \phi_1(\vec{x_1}) & \phi_2(\vec{x_1}) & ... & \phi_N(\vec{x_1}) \\ \phi_1(\vec{x_2}) & \phi_2(\vec{x_2}) & ... & \phi_N(\vec{x_2}) \\ \vdots & \vdots & \ddots & \vdots \\ \phi_1(\vec{x_N}) & \phi_2(\vec{x_N}) & ... & \phi_N(\vec{x_N}) \end{vmatrix} \tag{2.10}$$

Here $\phi_i(\vec{x_j})$ is ith one-electron spin orbital and $\vec{x_j} = (\vec{r_j}, \sigma_j)$ is spatial and spin coordinates of jth electron. The Hartree-Fock method is based on one-electron approach and it contains indistinguishable property of the electrons. If we adopt the form of solution, the Hartree-Fock energy becomes

$$E_{HF} = \langle \Phi_{HF} | \hat{H} | \Phi_{HF} \rangle =$$

$$\sum_{i=1}^{N} \int \phi_i^*(\vec{x}) \left[-\frac{\hbar^2}{2m} \nabla_i^2 - e^2 \sum_{I=1}^{P} \frac{Z_I}{|\vec{R_I} - \vec{r}|} \right] \phi_i(\vec{x}) d\vec{x} +$$

$$\frac{e^2}{2} \sum_{i=1}^{N} \sum_{j=1}^{N} (\iint \phi_i^*(\vec{x}) \phi_j^*(\vec{x'}) \frac{1}{|\vec{r} - \vec{r'}|} \phi_j(\vec{x'}) \phi_i(\vec{x}) d\vec{x} d\vec{x'} -$$

$$\iint \phi_i^*(\vec{x}) \phi_j^*(\vec{x'}) \frac{1}{|\vec{r} - \vec{r'}|} \phi_i(\vec{x'}) \phi_j(\vec{x}) d\vec{x} d\vec{x'}) + \frac{e^2}{2} \sum_{I=1}^{P} \sum_{J \neq I}^{P} \frac{Z_I Z_J}{|\vec{R_I} - \vec{R_J}|} \tag{2.11}$$

Using the variational principles, we can arrive at the Hartree-Fock equation

$$[-\frac{\hbar^2}{2m} \nabla_1^2 \phi_i(\vec{r}) - e^2 \sum_{I=1}^{P} \frac{Z_I \phi_i(\vec{r})}{|\vec{R_I} - \vec{r}|} + \left(e^2 \sum_{j=1}^{N} \int \frac{|\phi_j(\vec{r'})|^2}{|\vec{r'} - \vec{r}|} d\vec{r'} \right) \phi_i(\vec{r}) -$$

$$e^2 \sum_{j=1}^{N} \delta_{\sigma_i \sigma_j} \left(\int \frac{\phi_j^*(\vec{r'}) \phi_i(\vec{r'})}{|\vec{r'} - \vec{r}|} d\vec{r'} \right) \phi_j(\vec{r})] = E_i \phi_i(\vec{r}) \tag{2.12}$$

2.3.2 Density Functional Theory

2.3.2.1 Hohenberg-Kohn Theorem

With the Hohenberg-Kohn theorem, we can treat the external potential

$$V_{ext}(\vec{r}) \equiv -e^2 \sum_{I=1}^{P} \frac{Z_I}{\left|\vec{R_I} - \vec{r}\right|} \tag{2.13}$$

which arise from nucleus, equivalently as the ground state electron density.

$$\rho(\vec{r}) \equiv \sum_{i=1}^{N} \int \left|\Phi_{ground}(\vec{r_1}, ..., \vec{r_i} = \vec{r_1}, ..., \vec{r_N})\right|^2 d\vec{r_1} d\vec{r_{i-1}} d\vec{r_{i+1}} d\vec{r_N} \tag{2.14}$$

Here is the proof.

Assume that there is one same ground state electron density($\rho(\vec{r})$) for two different external potential($V_{ext}(\vec{r}), V_{ext}{}'(\vec{r})$) and their ground states(Φ, Φ'). Then

$$\begin{aligned} E_0 = \langle \Phi | \hat{H} | \Phi \rangle &< \langle \Phi' | \hat{H} | \Phi' \rangle = \langle \Phi' | \hat{H}' | \Phi' \rangle + \langle \Phi' | \hat{H} - \hat{H}' | \Phi' \rangle \\ &= E_0' + \int \rho(\vec{r}) \left(V_{ext}(\vec{r}) - V_{ext}{}'(\vec{r}) \right) d\vec{r} \end{aligned} \tag{2.15}$$

Equivalently,

$$\begin{aligned} E_0' = \langle \Phi' | \hat{H}' | \Phi' \rangle &< \langle \Phi | \hat{H}' | \Phi \rangle = \langle \Phi | \hat{H} | \Phi \rangle + \langle \Phi | \hat{H}' - \hat{H} | \Phi \rangle \\ &= E_0 - \int \rho(\vec{r}) \left(V_{ext}(\vec{r}) - V_{ext}{}'(\vec{r}) \right) d\vec{r} \end{aligned} \tag{2.16}$$

Therefore, if we add the inequalities (2.13) and (2.14), we get the contradiction $E_0 + E_0' < E_0' + E_0$. So we've prove one side of the above theorem using reduction to absurdity. The other side is easy to prove. Given external potential, by solving the Schrodinger's equation (2.6), we can get the ground state wave function and its electron density.

Using above theorem, we can conclude that as functional of electron density, we can get the ground state energy.

$$E_0 = E_0[\rho] \tag{2.17}$$

If we use electron density to get a electronic structure(the solution of the equation 2.6), it is called DFT(density functional theory) calculation.

2.3.2.2 Kohn-Sham Equation

Kohn and Sham thought that if we have non-interacting system that gives same electron density of interacting system, we can approximate the ground state energy. Therefore they assume the form of electron density

$$\rho(\vec{r}) = \sum_{i=1}^{N} \left|\phi_i(\vec{r})\right|^2 \tag{2.18}$$

then the Kohn-Sham energy becomes

$$E_{KS} = -\sum_{i=1}^{N} \frac{\hbar^2}{2m} \langle \phi_i | \nabla_i^2 | \phi_i \rangle - e^2 \sum_{I=1}^{P} \int \frac{Z_I}{\left|\vec{R_I} - \vec{r}\right|} \rho(\vec{r}) d\vec{r} + \frac{1}{2} \iint \frac{\rho(\vec{r'})\rho(\vec{r})}{\left|\vec{r'} - \vec{r}\right|} d\vec{r'} d\vec{r} + E_{XC} \tag{2.19}$$

Where E_{XC} is the exchange-correlation energy which is correction for the energy E_0 in equation (2.17). By variational principles the equation (2.19) becomes

$$-\frac{\hbar^2}{2m}\nabla^2\phi_i(\vec{r}) + \left[-e^2 \sum_{I=1}^{P} \frac{Z_I}{\left|\vec{R_I} - \vec{r'}\right|} + e^2 \int \frac{\rho(\vec{r'})}{\left|\vec{r'} - \vec{r}\right|} d\vec{r'} + \frac{\delta E_{XC}}{\delta \rho(\vec{r})}\right] \phi_i(\vec{r}) = E_i \phi_i(\vec{r}) \tag{2.20}$$

This is Kohn-Sham equation. We don't know the exact form of the $\frac{\delta E_{XC}}{\delta \rho(\vec{r})}$, and it's the one of the biggest topic today. The approximated

functional used in equation (2.20) determine the kind of DFT calculation.

LDA(local density approximation) and GGA(generalized gradient approximation) indicate the class of exchange-correlation functional. PBE(Perdew-Burke-Ernzerhof) functional and PW91(Perdew-Wang) functional are GGA class exchange-correlation functionals.

2.4 Bloch Theorem

Under a periodic potential ($U(\vec{r}) = U(\vec{r}+\vec{R})$ where $\vec{R}$ is a lattice vector), the single electron Schrodinger's equation

$$\left(-\frac{\hbar^2}{2m}\nabla^2 + U(\vec{r})\right)\psi(\vec{r}) = E\psi(\vec{r}) \tag{2.21}$$

can be transformed using the Fourier's transformation

$$\psi(\vec{r}) = \frac{1}{\sqrt{V}}\sum_{q}\psi(\vec{q})e^{i\vec{q}\cdot\vec{r}} \tag{2.22}$$

$$U(\vec{r}) = \sum_{K} U_{\vec{K}} e^{i\vec{K}\cdot\vec{r}} \tag{2.23}$$

$$\left(\frac{\hbar^2 q^2}{2m} - E\right)\psi(\vec{q}) + \sum_{\vec{K}} U_{\vec{K}}\psi(\vec{q}-\vec{K}) = 0 \tag{2.24}$$

Where $\vec{K}$ is reciprocal lattice vector. From equation (2.24), we arrive at

$$\psi_{\vec{k}}(\vec{r}) = \frac{e^{i\vec{k}\cdot\vec{r}}u_{\vec{k}}(\vec{r})}{\sqrt{N}} \tag{2.25}$$

Where $u_{\vec{k}}(\vec{r}) = u_{\vec{k}}(\vec{r}+\vec{R})$. That's Bloch's theorem.

2.5 Monte Carlo Simulation

Monte Carlo simulations use random number to simulate mathematical and physical system. In my case, I used Monte Carlo simulation to analysis systems in thermal equilibrium. Specifically I used metropolis algorithm.

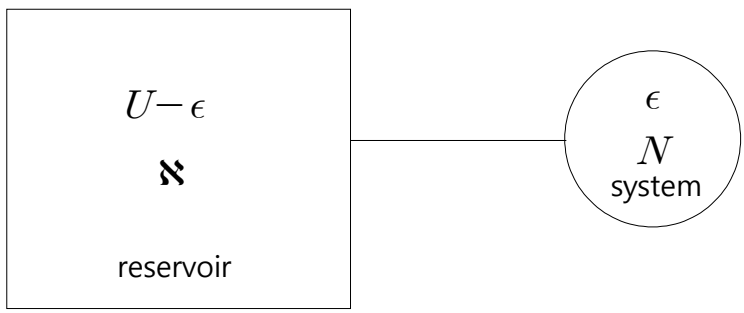

Figure 2.1 : Schematic diagram for canonical ensemble system.

For canonical ensembles

$$k_B \ln \Omega = S(U-\epsilon) = S(U) - \epsilon\left(\frac{\partial S}{\partial U}\right)_{\aleph, V} = S(U) - \frac{\epsilon}{T} \tag{2.26}$$

Where Ω is the number of microstate, S is the entropy, $\aleph$ is the number of particles in reservoir, N is the number of particles in the system, $U-\epsilon$ is the energy of reservoir, and ϵ is the energy of the system. Therefore, the probability that the system has the energy ϵ is

$$P(\epsilon) \propto \Omega = e^{\frac{S(U-\epsilon)}{k_B}} \propto e^{-\frac{\epsilon}{k_B T}} \tag{2.27}$$

Using the above result, we can construct metropolis algorithm for canonical ensembles. Here are the procedures.

1. Given temperature and total number of particles in the universe(system plus reservoir), randomly locate particles' positions in the universe.
2. Get the total energy of the universe.
3. Now, randomly choose one particle and randomly relocates its position in the universe.
4. Calculate the total energy, and compare the energy with previous configuration's total energy.
5. If the energy goes down, accept the new configuration, else call a random number $r \in (0,1)$. If $r \leq e^{\frac{|\Delta E|}{k_B T}}$ accept the new configuration, else go back the previous configuration.
6. Repeat the procedure 3~5 until the system's macroscopic variables converge.

Using the algorithm, we can analysis a system in thermal equilibrium.

Chapter 3
Calculation Result

3.1 Systems

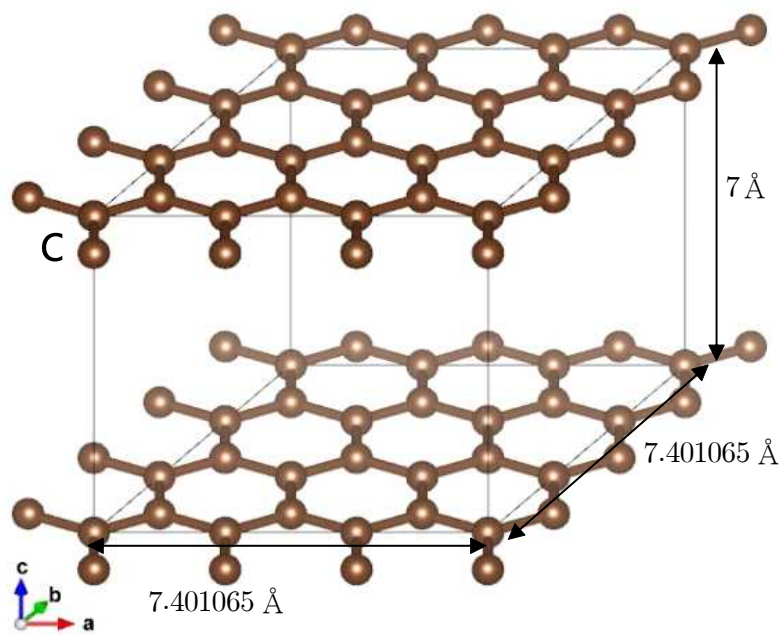

Figure 3.1: graphene layers

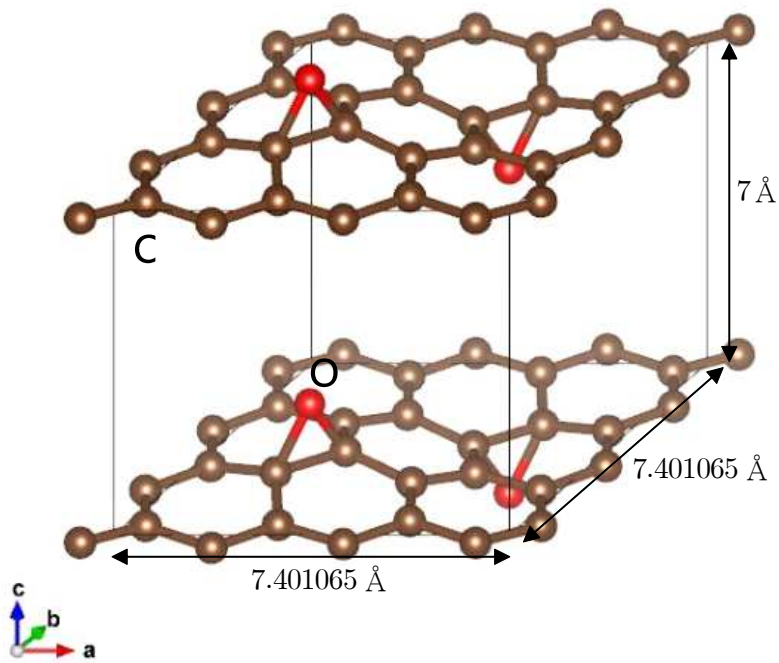

Figure 3.2: graphene oxide layers

Figure 3.1 and figure 3.2 show my systems, graphene layers and graphene oxide layers in which oxygens are attached to carbon as epoxy group. Layer spacing for both layers is 7 Å. Figure 3.1 and figure 3.2 were unit cells for DFT calculations and that are 3×3 times of graphene primitive unit cell in layer plane. For graphene oxide layer, the number ratio of oxygen to carbon is 1:9. The structure of graphene oxide layers is determined by ion-relaxed DFT

calculation. I analyzed how much H_2 will be stored in those two systems at room temperature($k_B T_R = 0.0258 eV$) and compared them.

3.2 $H_2 - H_2$ Interaction Energy

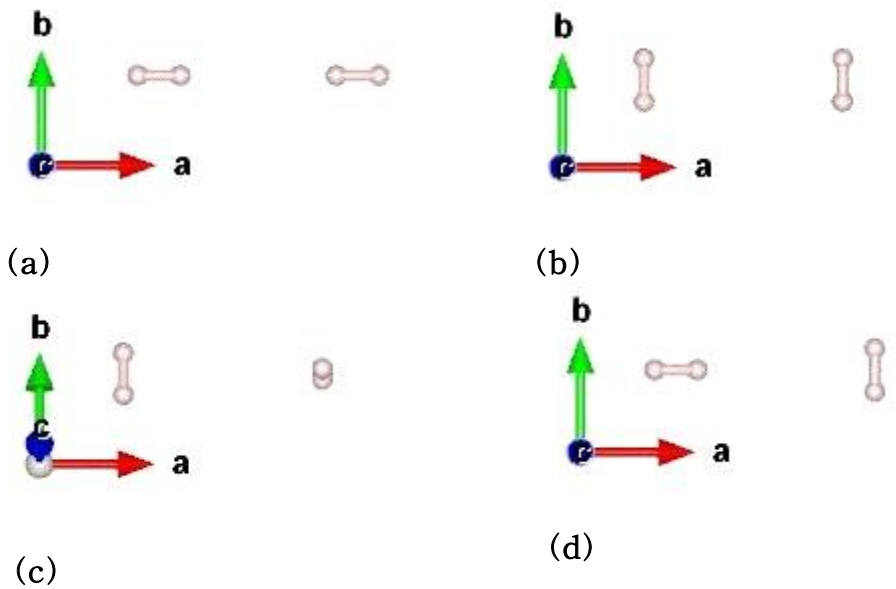

Figure 3.3: 4 most symmetric configuration for $H_2 - H_2$ interaction. (a) Horizontal (b) Parallel (c) Perpendicular (d) Vertical

Figure 3.3 shows the 4 most symmetric configuration for $H_2 - H_2$ interaction. For those configuration, I got the $H_2 - H_2$ interaction energy.

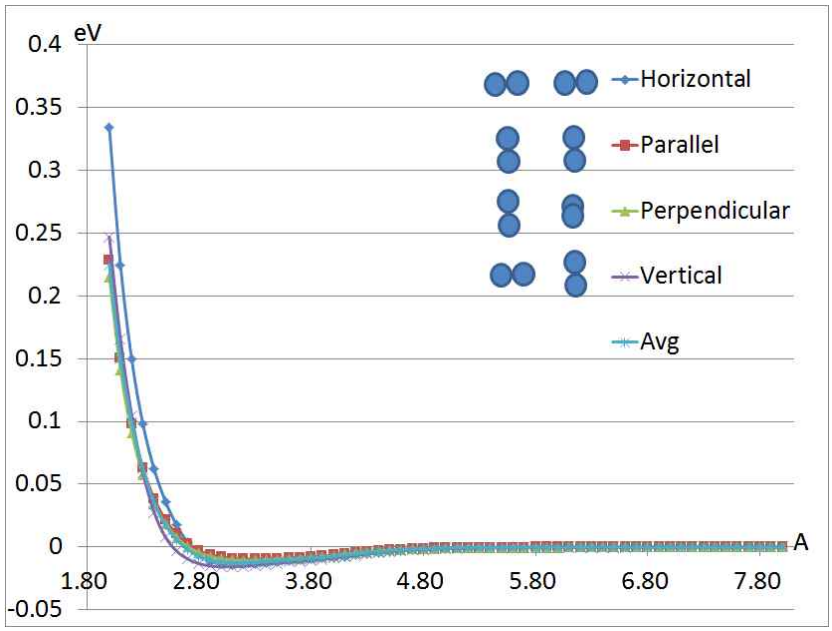

Figure 3.4: The $H_2 - H_2$ interaction energy graph.

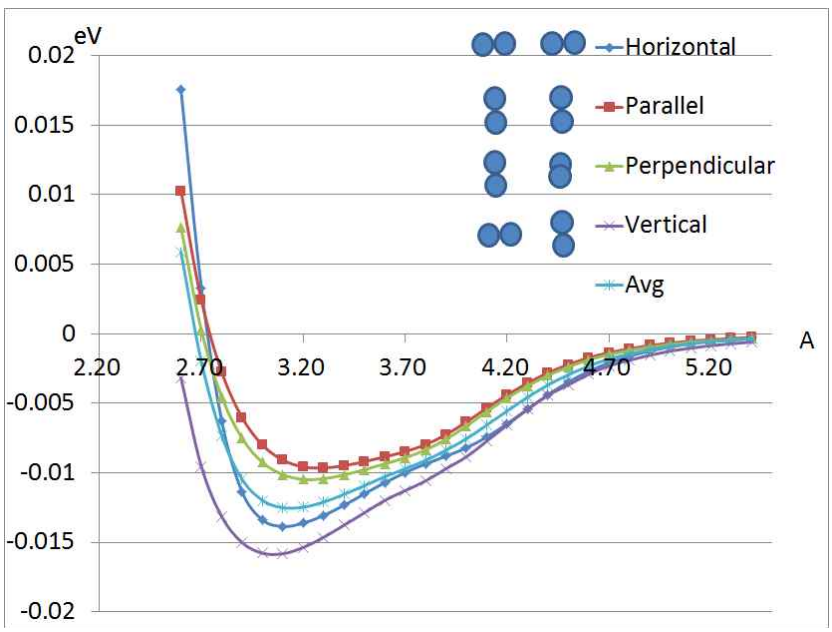

Figure 3.5: The $H_2 - H_2$ interaction energy graph which focuses on negative energy part of figure 3.4

Figure 3.4 and figure 3.5 show H_2-H_2 interaction energy graph. Increasing the distance between H_2's center from 2 Å to 8 Å by 0.1 Å, I got the results. This is the DFT calculation results. From the graph, we can see that the maximum energy difference between the different angles is about $0.005\,eV$. At the room temperature ($k_BT_R=0.0258\,eV$), the relative probability between angles is $e^{\frac{0.005}{0.0258}}\cong 1.12$, So we can ignore the angle dependence. The 'Avg' in the graphs is the result. I averaged out the H_2-H_2 interaction energy with the probability $e^{\frac{-E(eV)}{0.0258\,(eV)}}$ over the angles for each distance.

3.3 Potential Energy Field

Now for the systems, figure 3.1 and figure 3.2, I got the potential energy fields. The method is here. First, I divided the space that is between layers, as $9\times9\times9$ grid. Second, locate H_2 at a grid point in the direction of one of the system axes. Third, get the total energy by DFT calculations and subtract the reference energy which is the systems' total energy without H_2. Fourth, repeat the 2nd~3rd procedure over all grid points using symmetry of the systems to reduce the calculations for each axis directions and average out the angle dependence.

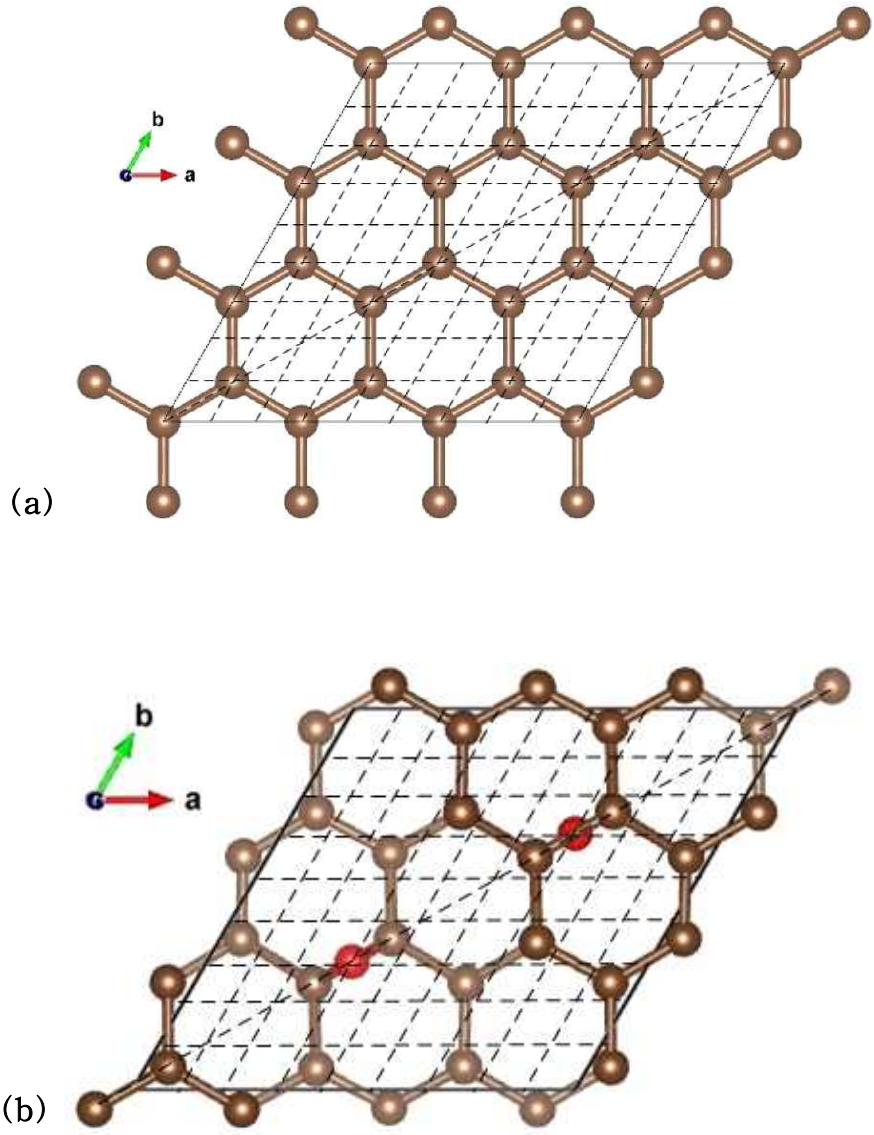

Figure 3.6: Grid in (a) graphene layers and (b) graphene oxide layers; top view.

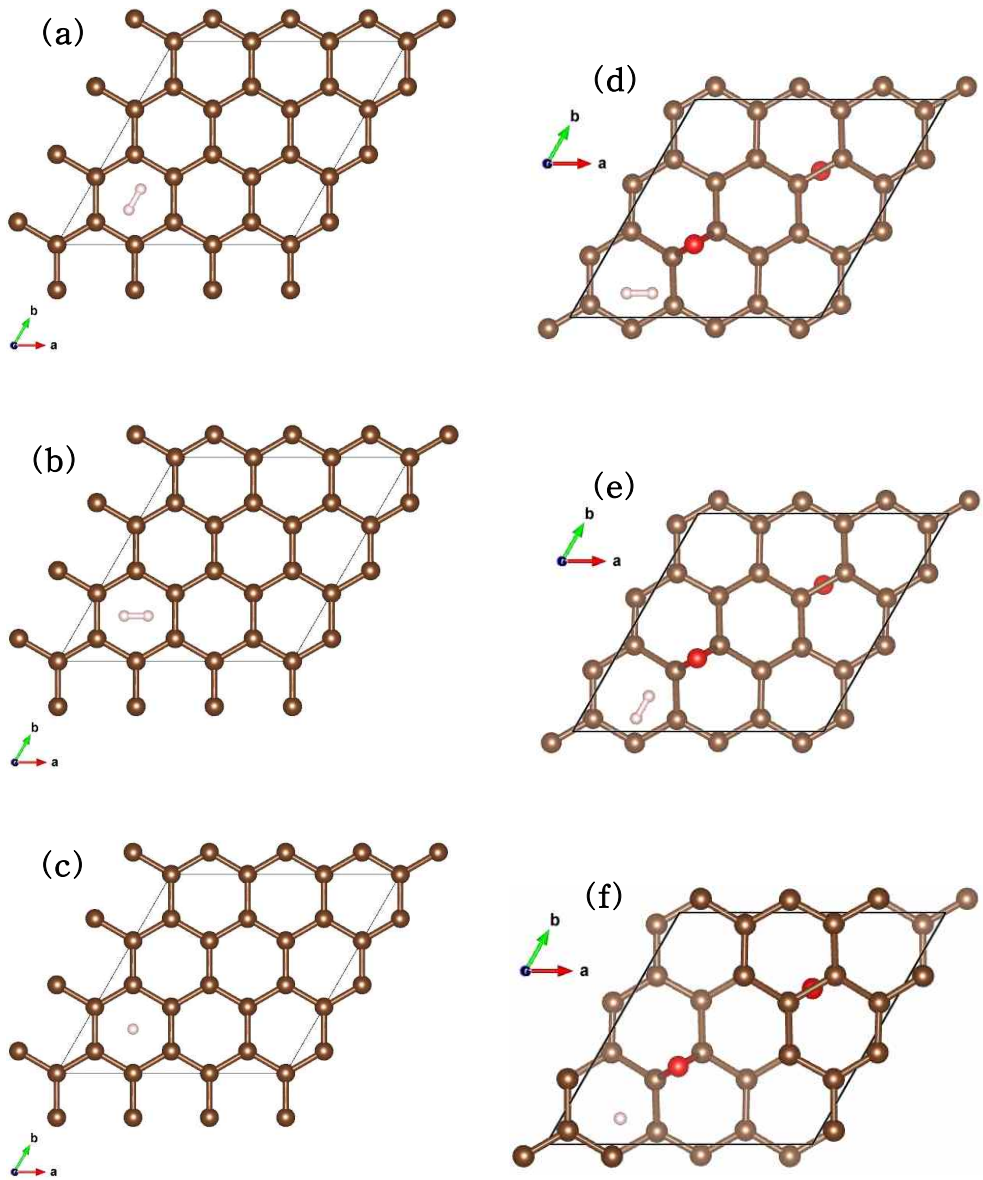

Figure 3.7: 3 axes directions of H_2 in graphene layers(a),(b),(c) and graphene oxide layers(d),(e),(f); top view.

3.3.1 Graphene Layers

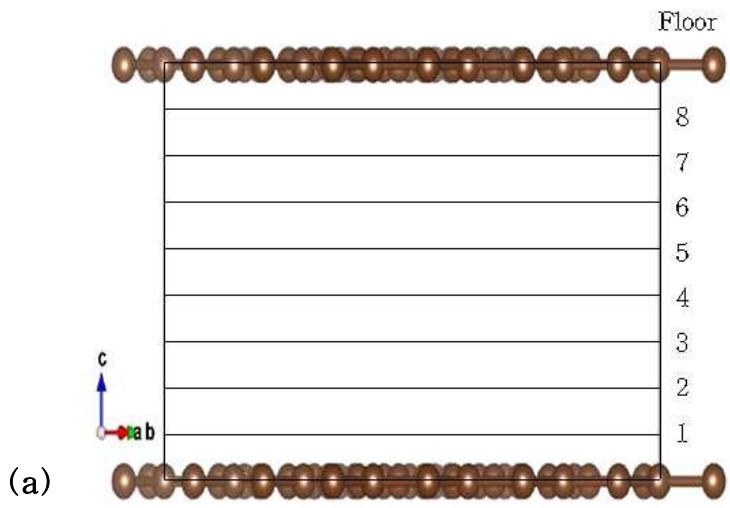

(a)

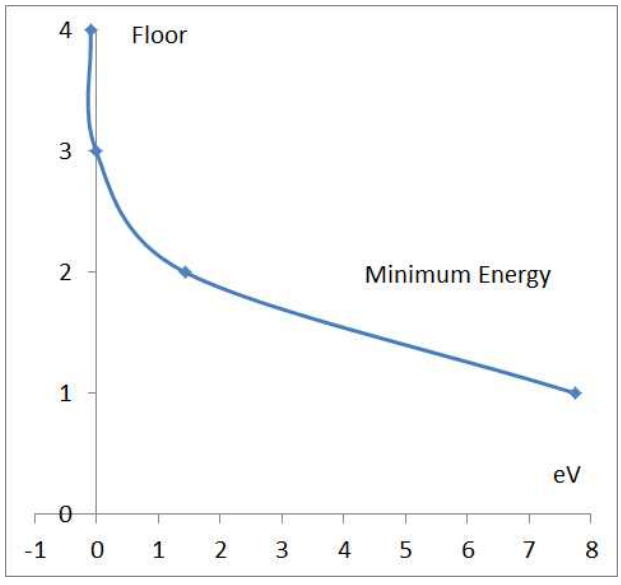

(b)

Figure 3.9: (a) Floors between graphene layers (b) Minimum energy at the floor over every grid points and angles of H_2.

Floor	Minimum Energy(eV)
4	-0.0962752
3	-0.00751314
2	1.42772991
1	7.73665513

Table 3.1: Minimum energy at the floors over every grid points and angles of H_2.

From table 3.1, we can know that hydrogen molecules don't enter the floor 1,2,8 and 9 because of the relative probabilities $e^{-\frac{7.736655}{0.0258}} \simeq (1.71\times10^{130})^{-1}, e^{-\frac{1.42773}{0.0258}} \simeq (1.08\times10^{24})^{-1}, (1.08\times10^{24})^{-1}$ and $(1.71\times10^{130})^{-1}$ with respect that H_2 is not enter the system, and we can know hydrogen molecules most probably enter between the floor 4 and 5.

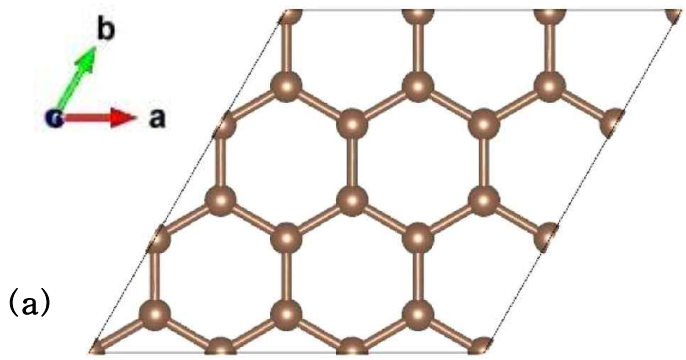

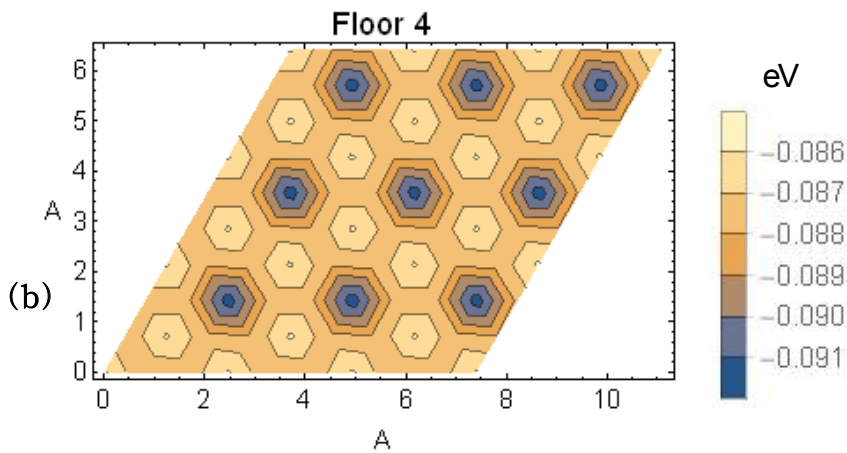

Figure 3.10: (a) the positions of carbons. Contour plots for graphene layers at (b) floor 4 where I thermally average out the angle dependence of H_2 at each grid points.

Figure 3.10 is the contour plots for floor 4. From there we can see that the potential energy field is smooth. Therefore H_2 has potential well rather than specific binding site. Using above data, we can draw schematic diagram for graphene layers. Figure 3.11 represents that. Hydrogen molecules strongly enter blue region and less enter the yellow region, and they are almost forbidden to enter the write region.

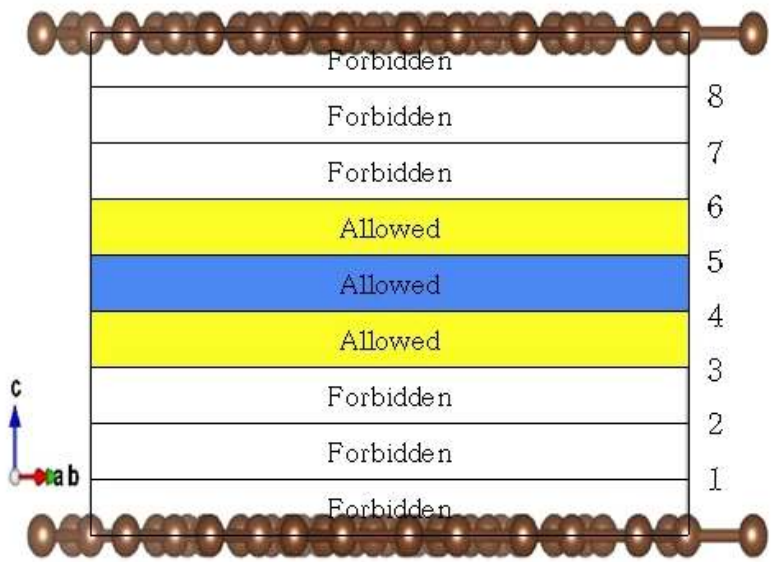

Figure 3.11: Schematic diagram for the grahene layers

3.3.2 Model System for the Graphene Layers

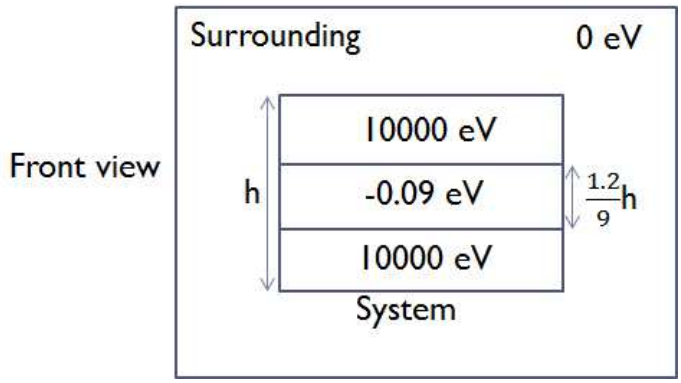

Figure 3.12: Model system for graphene layers

Using the previous data, we can construct model system for graphene layers. Figure 3.12 shows the model system for the graphene layers. We can calculate how much H_2 molecules enter the system without considering $H_2 - H_2$ interaction.

$$N_{out} : N_{in} = V_{out} : V_{in} \times \frac{1.2}{9} e^{\frac{0.09\,(eV)}{0.0258\,(eV)}} = V_{out} : 4.364\, V_{in} \tag{3.1}$$

This is simply thermodynamic relation using

$$N_{in} = \frac{\int \dots \int C_{in}(\{\vec{r_i}\}) e^{-(U_{K.E}(\{\vec{p_i}\}) + U_{P.E}(\{\vec{r_i}\}))/k_B T} d\vec{r_1} \dots d\vec{r_N} d\vec{p_1} \dots d\vec{p_N}}{\int \dots \int e^{-(U_{K.E}(\{\vec{p_i}\}) + U_{P.E}(\{\vec{r_i}\}))/k_B T} d\vec{r_1} \dots d\vec{r_N} d\vec{p_1} \dots d\vec{p_N}} \tag{3.2}$$

$$N_{out} = \frac{\int \dots \int C_{out}(\{\vec{r_i}\}) e^{-(U_{K.E}(\{\vec{p_i}\}) + U_{P.E}(\{\vec{r_i}\}))/k_B T} d\vec{r_1} \dots d\vec{r_N} d\vec{p_1} \dots d\vec{p_N}}{\int \dots \int e^{-(U_{K.E}(\{\vec{p_i}\}) + U_{P.E}(\{\vec{r_i}\}))/k_B T} d\vec{r_1} \dots d\vec{r_N} d\vec{p_1} \dots d\vec{p_N}} \tag{3.3}$$

Where $C_{in}(\{\vec{r_i}\})$ is a function that counts the number of particles in the system, and $C_{out}(\{\vec{r_i}\})$ is a function that counts the number of particles out of the system, i.e. in the surrounding.

3.3.3 Graphene Oxide Layers

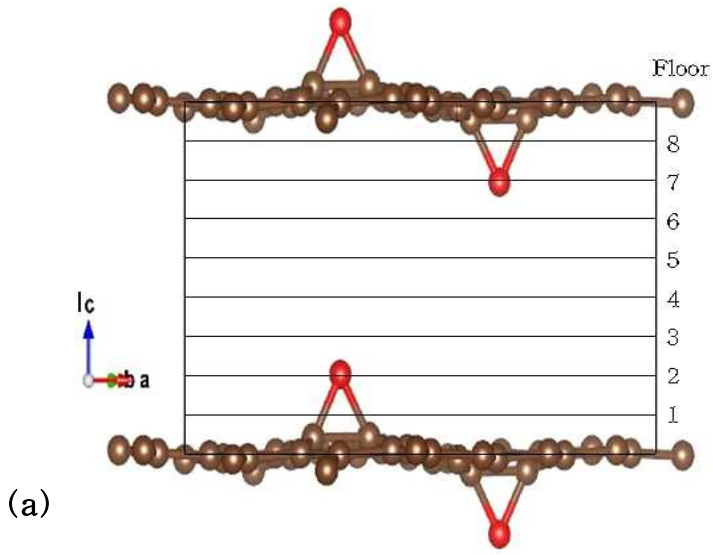

(a)

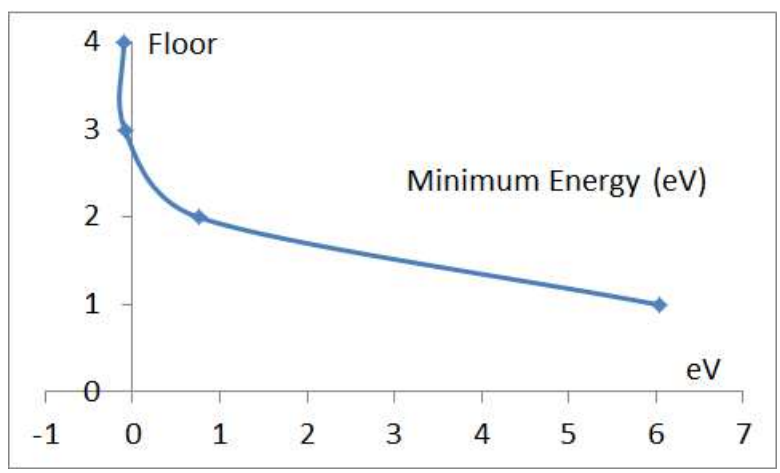

(b)

Figure 3.13: (a) Floors between graphene oxide layers (b) Minimum energy at the floors over every grid points and angles of H_2.

Floor	Minimum Energy(eV)
4	-0.10355716
3	-0.08713057
2	0.75868171
1	6.03136528

Table 3.2: Minimum energy at the floors over every grid points and angles of H_2.

Like graphene layers, by seeing the table 3.2, we can know that hydrogen molecules don't enter the floor 1,2,8 and 9 because of the relative probability $e^{-\frac{6.031365\,(eV)}{0.0258\,(eV)}} \simeq (3.36\times10^{101})^{-1}, e^{-\frac{0.758682\,(eV)}{0.0258\,(eV)}} \simeq (5.90\times10^{12})^{-1}, (5.90\times10^{12})^{-1}$ and $(3.36\times10^{101})^{-1}$ with respect that H_2 is not enter the system. We can know that the minimum energy decreases at floor 3 and floor 4 compared with graphene layers. Now consider the contour plots.

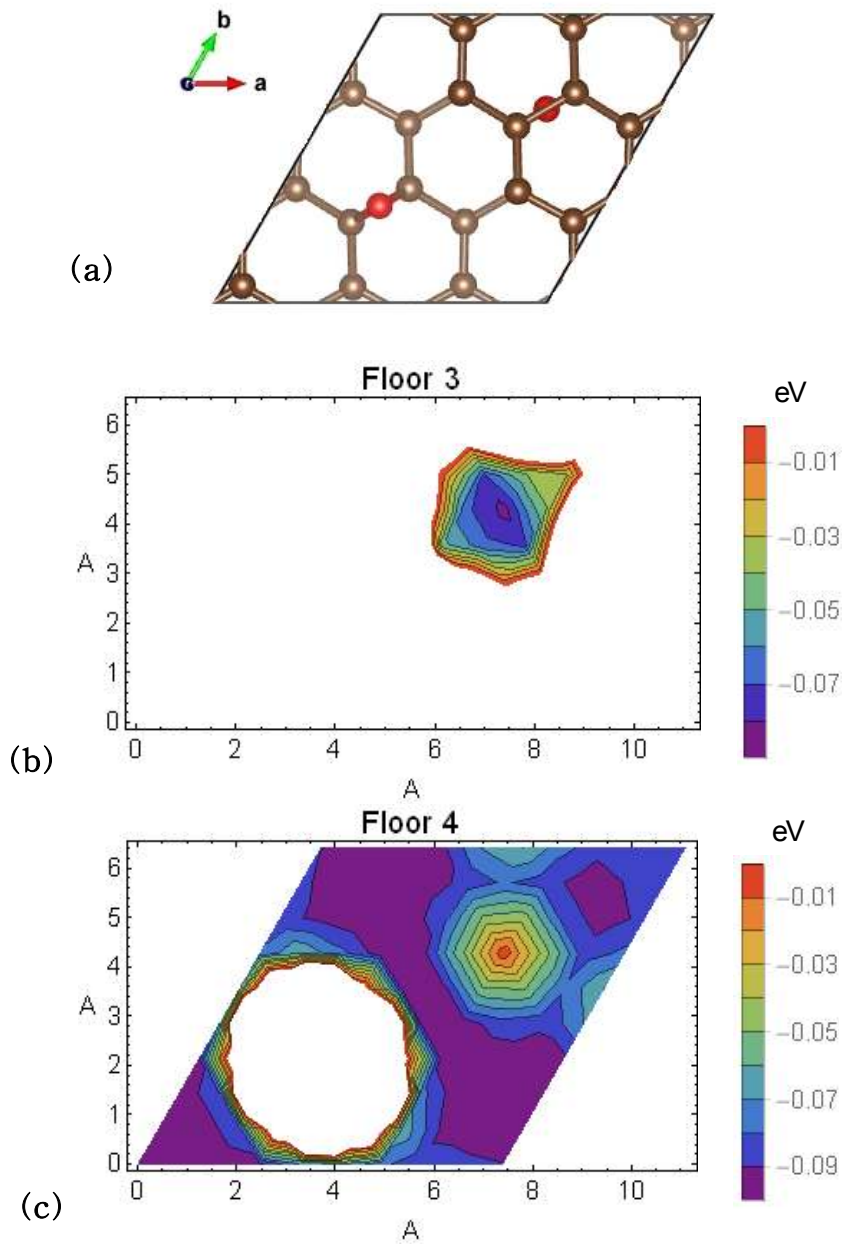

Figure 3.14: (a) the positions of carbons. Contour plots for graphene oxide layers at (b) floor 3 and (c) floor 4 where I thermally average out the angle dependence of H_2 at each grid points.

From figure 3.14(c), we can see that in the vicinity of oxygen the potential energy is high, so H_2 is prevented to go there. Unlike graphene layers where the potential is almost positive at floor 3, we can see the negative potential energy region at floor 3. Let's compare the contour plots at floor 4 between graphene layers and graphene oxide layers, it shows that away from the oxygen the potential energy is dropped.

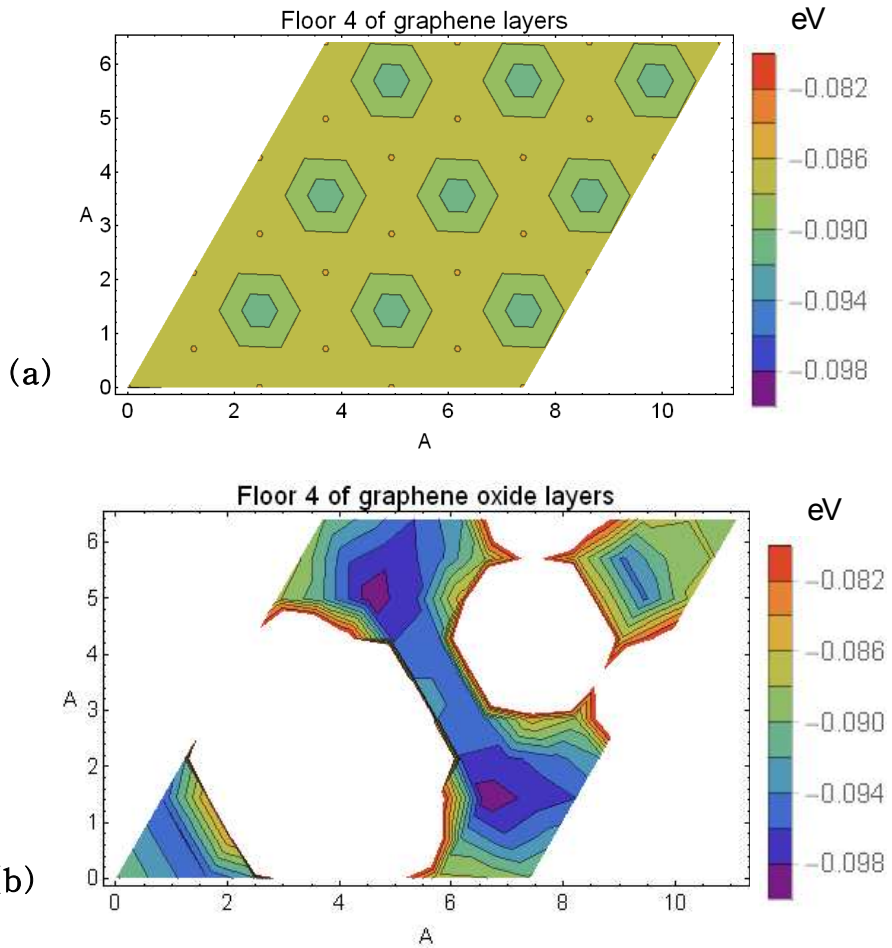

Figure 3.15: Contour plots at floor 4 for (a) graphene layers and (b) graphene oxide layers; contour is re-colored from above contour plots

Therefore, the oxygen partially prevents H_2 to enter the system, but partially help to enter the system.

Like graphene layers case, I can draw schematic diagram for graphene oxide layers. Figure 3.16 is the diagram where I write 'partially allowed' because in the vicinity of oxygens, the potential rise preventing H_2 from approaching.

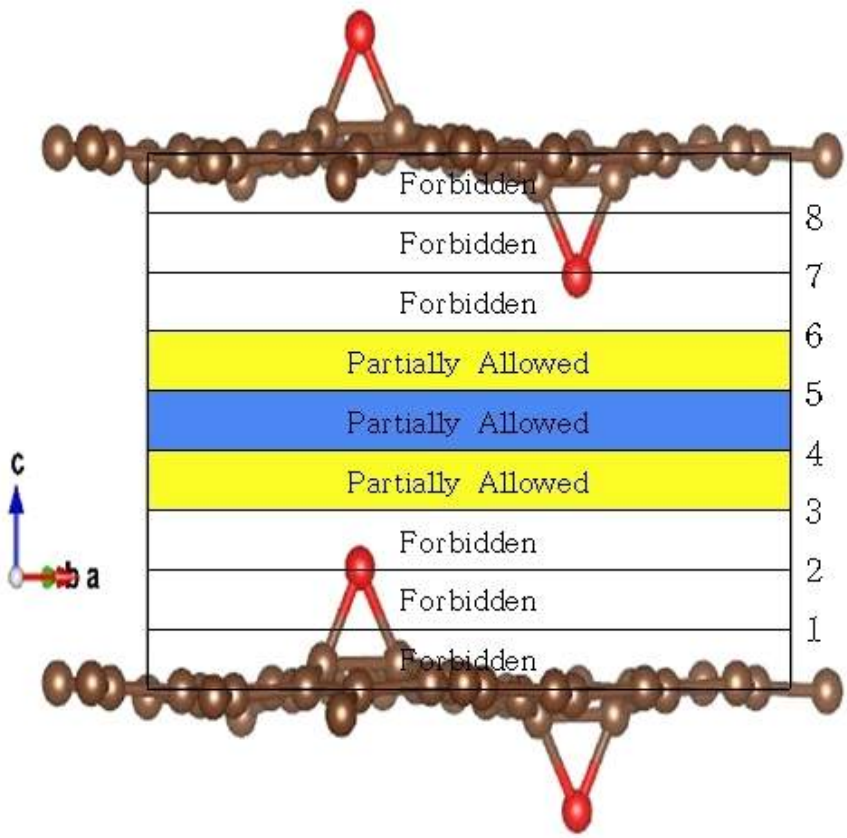

Figure 3.16: Schematic diagram for the grahene oxide layers

3.4 Monte Calro Simulations

I made Monte Carlo simulation program using Fortran 90. The program read 1) $H_2 - H_2$ interaction potential energy and 2) potential energy field of the systems. I set the surrounding to be 7 times the systems, i.e. the universe is 2^3 times the system.

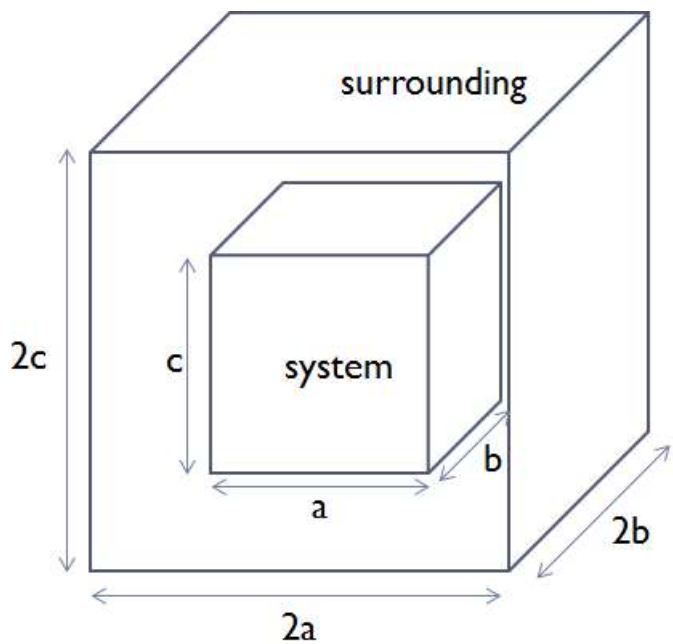

Figure 3.17: Monte Carlo simulation environment

There is a problem to use the above potential energy fields directly. Because previous systems has the volume $7.401065 \times \frac{1}{2} 7.401065 \times 7 (\text{Å}^3) = 332.0604 (\text{Å}^3)$ and the surrounding has the volume $2324.423 (\text{Å}^3)$, if a few of particles enter the system or surrounding, the pressure is too high with respect to the 1 atm. Because I want to simulate around from 1 atm. We need to enlarge the system. So, I enlarged the systems 6 times for each axis.

Nin	Pin (atm)
1	122.86
2	245.71
3	368.57
4	491.42
5	614.28
6	737.14
7	859.99
8	982.85
9	1105.70
10	1228.56

Nout	Pout (atm)
1	17.55
2	35.10
3	52.65
4	70.20
5	87.75
6	105.31
7	122.86
8	140.41
9	157.96
10	175.51

Table 3.3-left (3.4-right): The pressure of the system(surrounding) corresponding the number of particle in the system(surrounding); The pressure is acquired by ideal gas law $PV = Nk_BT$ because in the range of the above table, the interaction is negligible.

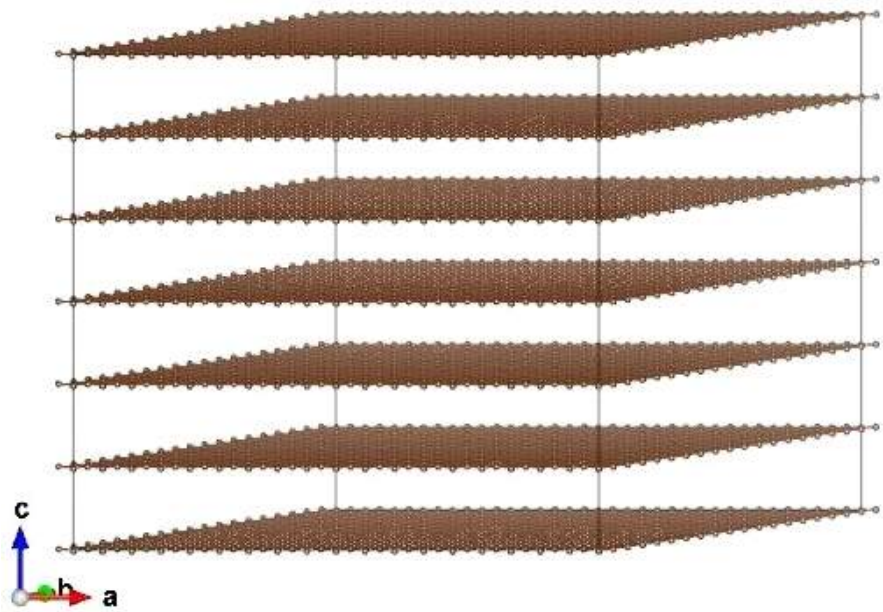

Figure 3.18: Enlarged system; graphene layers

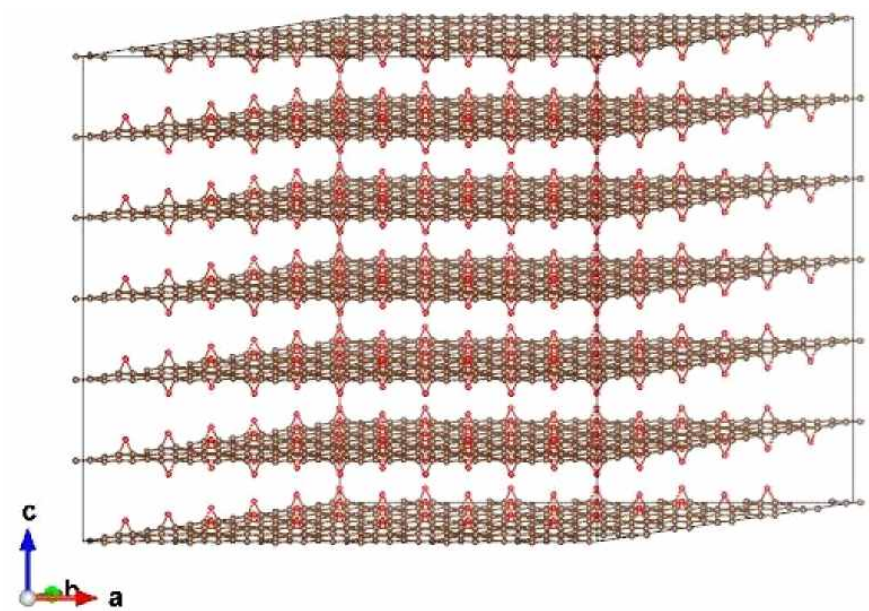

Figure 3.19: Enlargend system; graphene oxide layers

Figure 3.18 and Figure 3.19 show the enlarged systems. Therefore, the potential energy field corresponding the enlarged systems are true input for the Monte Carlo simulations.

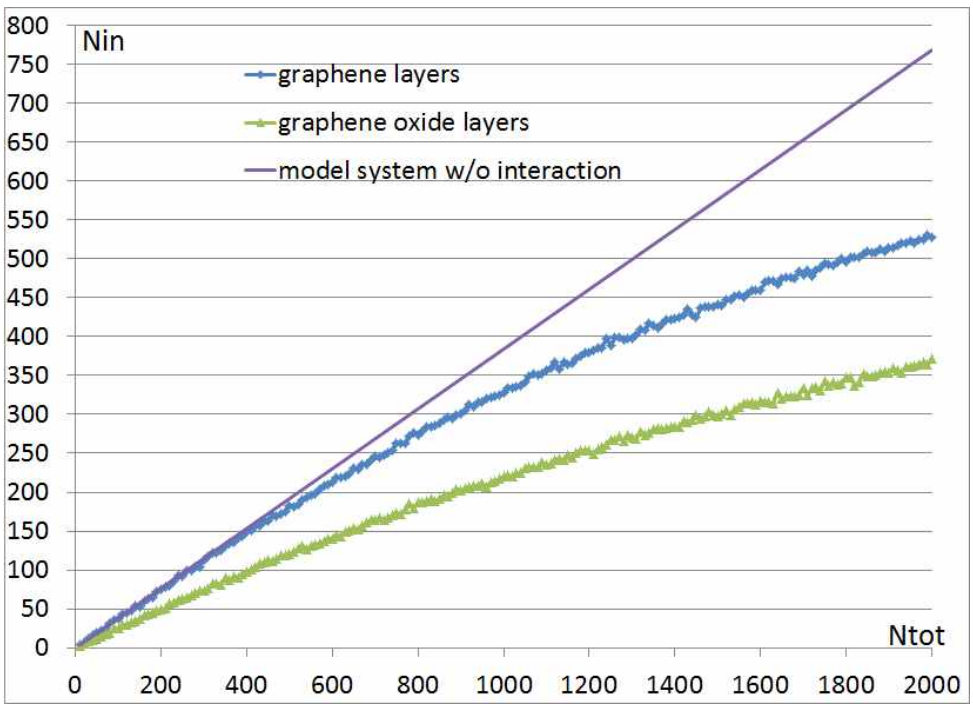

Figure 3.20: Total number of particle versus the number of particle in the systems.

Figure 3.20 is the results of Monte Carlo Simulation. From this figure we can see that the model system we've constructed at section 3.3.2 is the most powerful for hydrogen storage and the graphene oxide layers doesn't store hydrogen molecules than graphene layers

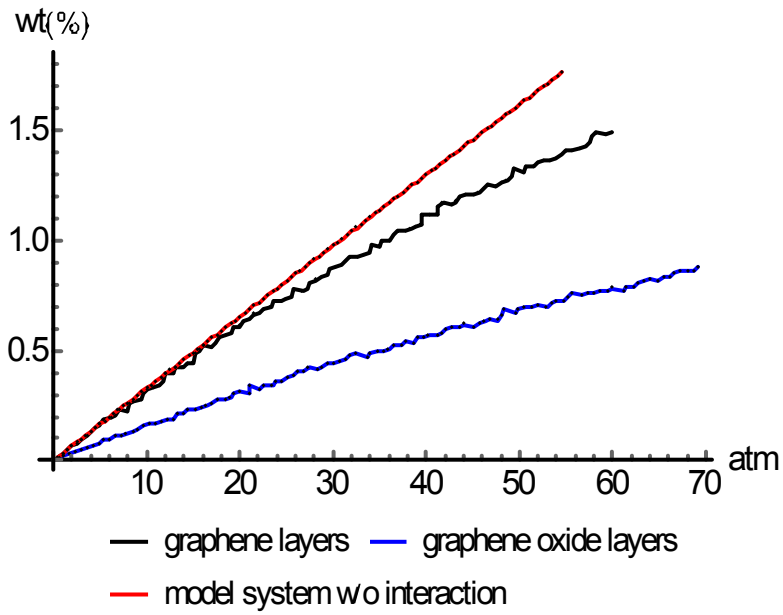

Figure 3.21: Pressure versus weight percent graph from 0 to 70 atm.

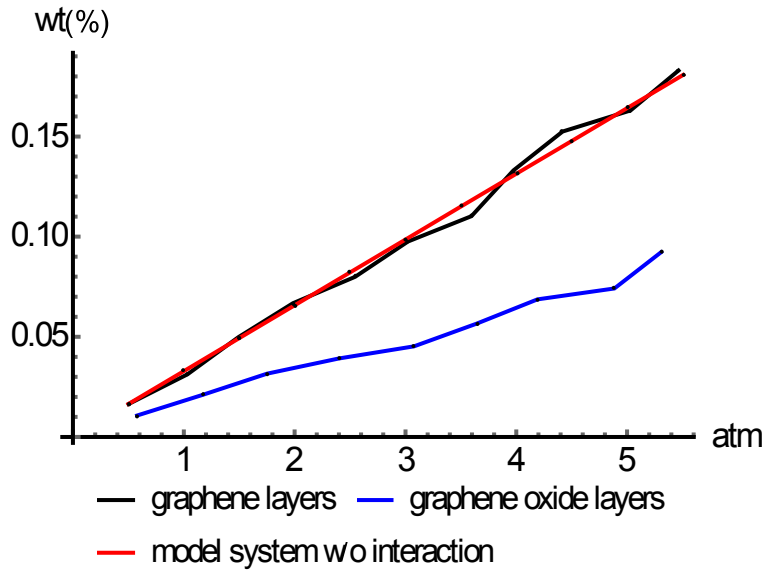

Figure 3.22: Pressure versus weight percent graph from 0 to 6 atm.

Figure 3.21 and 3.22 are pressure versus weight percent graphs where the pressure means surrounding's H_2 pressure. The weight percent is defined by

$$\frac{H_2\ mass\ (in\ the\ system)}{system\ mass + H_2\ mass\ (in\ the\ system)} \times 100(\%) = wt(\%) \quad (3.4)$$

From the result, we can know that at 10 atm, the weight percent are 0.31 wt(%) for graphene layers and 0.16 wt(%) for graphene layers and at 50 atm, 1.3 wt(%) for grapehen layers and 0.68 wt(%) for graphene oxide layers. The weight percents for graphene oxide layers are about the half of that for graphene layers.

Chapter 4
Calculation Details

4.1 VASP Options

- The unit cells are figure 3.1 and 3.2 where a hydrogen molecule is added on a grid point in the one of the axes directions.
- Energy cutoff for plane wave basis set is $450 eV$. (ENCUT)
- Kinetic energy cutoff for the augmentation charges is $600 eV$. (ENAUG)
- Criteria for self-consistence loop for electronics structure is 10^{-5}. (EDIFF)
- Methfessel-Paxton smearing of order 1 with width $0.1 eV$ is used. (ISMEAR and SIGMA)
- Monkhorst-Pack sampling with no shift is used for k sampling for $10 \times 10 \times 2$ grid.
- GGA PBE functional is used.

4.2 Monte Carlo Simulation Options

1. I increased the total number of particles from 10 to 2000 by 10.
2. Iteration number for the Monte Carlo simulation is $total\ particle\ number \times 500$.
3. I repeated the Monte Carlo simulation 24 times and averaged them.

Chapter 5
Conclusions

Using ab-initio calculations and Monte Calro simulations, I semi-classically examined the hydrogen storage in graphene layers and graphene oxide layers. The graphene which give Novel price to Andre Geim and Konstantin Novoselov in 2010 is promising material for the future industry. However, it doesn't satisfactorily store the hydrogen molecule.(Note that the 2015 goal of U.S. Department of Energy is 6 wt(%)) Oxygen in graphene layers has two effect for the hydrogen storage. In the vicinity of oxygen, it occupies space disturbing hydrogen to enter the system, but away from the oxygen it drops the potential energy so, it helps the hydrogen to enter the system. The conflicting effects for hydrogen storage sum up as negative effect, that is, it disturbs hydrogen storage.

However, I analyzed the systems that have the layer spacing fixed in 7Å. If there are some effect about the layer spacing, there would be another results. From the schematic diagram, we can assume them. If we can have increased layer spacing, the negative potential energy region will be expand and the effect of the potential energy drop from oxygen will be increase even though the space occupying effect of oxygen is limited. Therefore, the total effect of oxygen may be changed.

Bibliography

[1] David S. Sholl and Janice A. Steckel, *DENSITY FUNCTIONAL THEORY: A Practical Introduction*, John Wiley & Sons, Hoboken (2009)

[2] Jorge Kohanoff, *Electronic Structure Calculations for Solids and Molecules:* Theory and Computational Methods, Cambridge University Press, Cambridge (2006)

[3] Michael P. Marder, *Condensed Matter Physics*, 2nd ed, John Wiley & Sons, Hoboken (2010)

[4] Stephen J. Blundell and Katherine M. Blundell, *Concepts in Thermal Physics*, 2nd ed, Oxford University Press, New York (2010)

[5] R. M. Martin, *Electronic structure: Basic theory and practical methods*, Cambridge University Press, Cambridge (2004)

[7] Charles Kittel, *Introduction to Solid State Physics*, 8th ed, John Wiley & Sons, Hoboken (2005)

[8] Leonard I. Schiff, *Quantum Mechanics*, 3rd ed, McGraw-Hill, New

York (1968)

[9] Larry R. Nyhoff and Sanford C. Leestma, *Introduction to Fortran 90 for Engineers And Scientists*, Prentice Hall, New Jersey (1996)

[10] Neil W. Ashcroft and N. David Mermin, *Solid State Physics*, Cengage Learning, Boston (1976)

[11] P. Hohenberg and W. Kohn, Phys. Rev. **136** B806 (1964)

[12] J. P. Perdew, K. Burke, and M. Ernzerhof, Phys. Rev. Lett. **77**, 3865 (1996).

[13] Hoonkyung Lee, Woon Ih Choi, and Jisoon Ihm, Phys. Rev. Lett. **97**, 056104 (2006)

[14] http://en.wikipedia.org/wiki/Hydrogen_storage [Dec. 15, 2014]

국문 초록

화석에너지의 고갈과 환경오염으로 새로운 대체에너지의 개발이 각광받고 있다. 그중 수소는 물에서 쉽게 얻을 수 있다는 점과 환경오염 물질을 방출하지 않는 다는 점에서 가장 촉망 받고 있는 에너지원 중 하나이다. 하지만 수소를 실질적인 에너지원으로 사용함에 있어 몇 가지 문제가 있는데, 그중 가장 중요한 것이 가능한 많은 수소를 안정하게 저장하는 기술이다.

2010년 영국의 가임과 노보셀로프는 그래핀을 만드는데 성공한 공로로 노벨물리학상을 수상하였다. 그래핀은 탄소원자가 2차원으로 배열된 물질로서 높은 강도와 높은 전기전도도등 그 특이성으로 인해 현재 활발히 연구가 진행되고 있는 물질이며 이 논문에서는 그래핀층과 산소가 에폭시기로 도핑 된 산화그래핀층 사이에 수소가 들어갔을 때, 그 에너지 변화를 이론적으로 계산해보고 이를 토대로 그래핀층과 산화그래핀층에서 수소저장량을 계산해보았다.

계산에는 두 가지 방법의 쓰였다. 하나는 밀도범함수이론을 사용한 제일원리계산이며, 두 번째는 몬테카를로 시뮬레이션이다. 밀도범함수이론은 전자의 밀도로 물질의 전자구조를 기술하는 이론으로 다음과 같은

$$-\frac{\hbar^2}{2m}\nabla^2\phi_i(\vec{r})+\left[-e^2\sum_{I=1}^{P}\frac{Z_I}{\left|\overrightarrow{R_I}-\overrightarrow{r'}\right|}+e^2\int\frac{\rho(\overrightarrow{r'})}{\left|\overrightarrow{r'}-\vec{r}\right|}d\overrightarrow{r'}+\frac{\delta E_{XC}}{\delta\rho(\vec{r})}\right]\phi_i(\vec{r})=E_i\phi_i(\vec{r})$$

Kohn-Sham 방정식을 품으로써 계산을 한다. 제일원리계산은 VASP(Vienna Abinitio Simulation Package)를 사용하였으며 PBE(Perdew, Burke and Ernzerhof) 범함수를 사용하였다.

정준집합에 대한 몬테카를로 시뮬레이션은 다음과 같다. 시스템에 여러 개의 입자를 랜덤하게 위치시킨다. 그런 후 하나의 입자를 임의로 선택하여 랜덤하게 위치를 바꾼다. 바뀐 상태가 이전 상태보다 에너지가 낮아지면 허용하고, 에너지가 올라가면 $\exp(-\frac{|\Delta E|}{k_BT})$의 확률로 바뀐 상태를 허용한다. 이런 시행을 많이 반복하면 시스템은 열역학적으로 평형에 이른다. 이 몬테카를로 시뮬레이션은 포트란90으로 직접 코드를 작성하

여 수행하였다.

계산의 순서는 다음과 같다. 첫 번째로 수소분자 2개에 대해 수소와 수소 간 거리에 따른 에너지를 계산한다. 수소는 이원자분자로 수소 간 에너지는 거리뿐만 아니라 각 분자의 공간상 방향에도 영향을 받는다. 그렇지만 방향성에 의존하는 에너지를 사용하면 계산의 양이 급격히 증가할 뿐 아니라, 방향성에 따른 에너지 차이가 작기 때문에 가장 대칭성을 크게 가지는 4가지 위치관계에 대해 에너지를 구하고, 이들의 열역학적 평균값을 수소 간 에너지로 사용하였다.

두 번째로 수소분자 하나가 그래핀층과 산화그래핀층 사이에 들어갔을 때 에너지를 각 위치에 대해 구함으로 에너지장을 구한다. 위와 마찬가지로 에너지장은 각 위치에서 수소의 방향성에 의존하는데 방향성을 제거하기 위해, 수소의 방향을 시스템의 세가지 축방향으로 두어 계산을 한 뒤 열역학적으로 평균을 냈다.

마지막으로 위에서 구한 정보들을 가지고 몬테카를로 시뮬레이션을 한다. 그러면 시스템 외부의 수소분자밀도와 시스템 내부의 수소분자밀도 관계를 수치적으로 구할 수 있는데, 이를 토대로 주어진 온도와 압력하에서 얼마만큼의 수소분자가 그래핀이나 산화그래핀층 사이에 저장되는지 구할 수 있다.

수소가 그래핀층 사이나 산화그래핀층 사이에 들어갔을 때, 특정 위치에 붙는 것이 아니라 전반적인 위치에서 에너지가 낮아진다. 이는 기존에 수소저장물질이 가지던 물리흡착과는 다른 현상으로 가스-가스 상변화를 통한 현상이며 열역학적으로 다뤄야 한다. 산소 도핑은 특정영역은 에너지를 낮춰주어 수소가 더 많이 저장되도록 하지만 산소 원자 근방은 에너지를 높여주어 수소가 들어오는 것을 막는다. 몬테카를로 시뮬레이션을 통해 우리의 시스템에서 산소 도핑의 효과가 결과적으로 수소 저장을 방해함을 확인할 수 있었다.

주요어: 수소 저장, 그래핀, 산화그래핀, 몬테카를로 시뮬레이션, 밀도범함수 이론
학번: 2013-20366